

# Averaged electron collision cross sections for thermal mixtures of $\beta$ -alanine conformers in the gas phase

Milton M. Fujimoto<sup>1,3</sup>, Erik V. R. de Lima<sup>1</sup> and Jonathan Tennyson<sup>2</sup>

<sup>1</sup>Departamento de Física, Universidade Federal do Paraná, 81531-990 Curitiba, PR, Brazil

<sup>2</sup>Department of Physics & Astronomy, University College London, Gower St., London, WC1E 6BT, UK

E-mail: <sup>3</sup>[milton@fisica.ufpr.br](mailto:milton@fisica.ufpr.br)

## Abstract.

A theoretical study of elastic electron scattering by gas-phase amino acid molecule  $\beta$ -alanine ( $\text{NH}_2\text{-CH}_2\text{-CH}_2\text{-COOH}$ ) is presented. R-matrix calculations are performed for each of the ten lowest-lying, thermally-accessible conformers of  $\beta$ -alanine. Eigenphase sums, resonance features, differential and integral cross sections are computed for each conformer. The positions of the low-energy shape resonance associated with the unoccupied  $\pi^*$  orbital of the  $-\text{COOH}$  group are found to vary from 2.5 eV to 3.3 eV and the resonance widths from 0.2 eV to 0.5 eV depending on the conformation. The temperature-dependent population ratios are derived, based on temperature-corrected Gibbs free energies. Averaged cross sections for thermal mixtures of the 10 conformers are presented. A comparison with previous results for the  $\alpha$ -alanine isomer is also presented.

## 1. Introduction

$\beta$ -alanine (3-aminopropanoic acid,  $\text{NH}_2\text{-CH}_2\text{-CH}_2\text{-COOH}$ ) is the simplest  $\beta$ -amino acid; it is an isomer of  $\alpha$ -alanine in which the amino group is bonded at the  $\beta$  carbon with the respect of carboxylic group ( $-\text{COOH}$ ).  $\beta$ -alanine is found in the interstellar medium and is most abundant amino acid in carbonaceous meteorites (IC chondrites) (Ehrenfreund et al. 2001). Gas-phase reaction studies show that it can be produced preferentially compared to  $\alpha$ -alanine (Blagojevic et al. 2003). Biological interest in  $\beta$ -amino acids has increased in the recent years due to applications in many research areas of medicine and chemistry (Juaristi & Soloshonok 2005).  $\beta$ -alanine occurs naturally in human tissue and mammalian, such as brain and liver, and insect cuticles, as well as, in plants and fruits (Kasschau et al. 1984). Despite  $\beta$ -amino acids not forming building blocks of proteins,  $\beta$ -alanine can be converted to  $\alpha$ -alanine enzymatically (Hayashi et al. 1961).  $\beta$ -alanine exist in central nervous system (CNS) in low concentration and there are some suggestions that it could be designated as a neurohormone (Choquet & Korn 1988) and others as a neurotransmitter (Tiedje et al. 2010).

In general, amino acids in solid phase or in aqueous environment are found in zwitterionic form ( $\text{NH}_3^+\text{-R-COO}^-$ ); however, as isolated molecules in the gas phase they are generally detected in their neutral structure ( $\text{NH}_2\text{-R-COOH}$ ). Amino acids are very flexible molecules:  $\beta$ -alanine has various singles chemical bonds which can freely rotate and can therefore generate numerous stable conformations, see Figure 1. Intramolecular interactions, such as H bonds, are important for determining the relative stability of these conformers and the geometries. A detailed discussion of the low-lying conformers of  $\beta$ -alanine is given in the next section.

There appears to be no published theoretical or experimental data on cross sections for electron collisions by  $\beta$ -alanine molecules. Recently we performed an R-matrix study of low-energy electron scattering by  $\alpha$ -alanine conformers in the gas phase (Fujimoto et al. 2016). This study demonstrated that for comparison with gas-phase measurements the theoretical cross sections should be calculated as an average of cross sections of individual conformers weighted by its respective population ratio in the molecular beam at the temperature at which the experiment is performed. Amino acids, in general, are very flexible molecules and in the gas phase they are found in many neutral conformational forms. Our study on  $\alpha$ -alanine showed that electron collision cross sections for specific conformation can be very different from those found for other conformers. This is particularly true if there are large differences in the permanent dipole moment between conformers.

A motivation for this study concerns DNA degradation by interaction with low-energy secondary electrons. Since the remarkable work of Boudaïffa et al. (2000) who demonstrated plasmid DNA exposed to an electron beam with energy less than 20 eV could induce single and double strand brake on DNA molecules, interest in electron collisions with biological molecules has grown considerably. The mechanism of DNA damage is associated with electron attachment. Here the electron is captured, generally

in an unoccupied orbital of some DNA building block, and forms a transient anion, called a resonance state. This temporary anion state can then decay into negative and neutral fragments. Knowledge about resonances associated with building blocks provides useful information for describing to fragmentation pathways.

In this work we present another study of low-energy electron collisions with molecules of biological interest, namely conformers of  $\beta$ -alanine. This molecule is thought to have many conformers in the gas phase; we focus on the 10 low-energy conformers which each should be present in significant quantity in the gas phase at a given temperature due to their low energy relative to lowest conformer. For each of these conformers we calculate the individual cross sections. Temperature-dependent averaged cross sections are computed by weighting each conformer cross section by its populations at the given temperature. Resonance features are discussed for each conformers.

The organization of article is as follows: section 2 presents a survey of what is know about the gas-phase conformers of  $\beta$ -alanine; section 3 gives an outline of the theory and details of the calculations. Section 4 presents and discusses our calculated data; this is followed by a summary of conclusions.

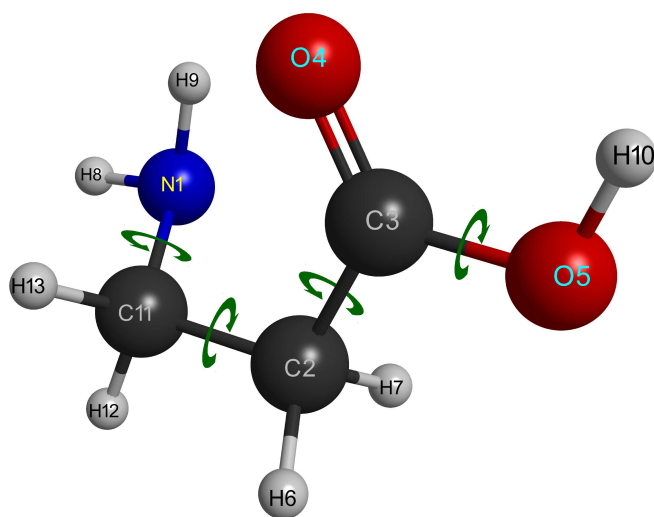


**Figure 1.** Structure of  $\beta$ -alanine. This amino acid is very flexible; the rotation of various bonds indicated generates many different conformers. (Figure generated with help of MacMolplt software (Bode & Gordon 1998))

## 2. Conformers

As we are interested in studying the amino acid in the gas phase, we survey available theoretical and experimental studies about  $\beta$ -alanine conformers. The first structure calculation of  $\beta$ -alanine conformations that we are aware of was made by Ramek (1990),

who performed calculations at the self-consistent field (SCF) level using a 4-31G split valence basis set and found 20 geometries which gave unique local minima in the potential energy surfaces. Ramek designated each unique structures as I, II, III etc following their relative energies, where conformer I is the lowest-energy structure. This nomenclature has been generally adopted and is used by us here. Ramek's structural analysis indicated that intramolecular interactions, such as hydrogen-bonding, give stability to the conformers. Ramek et al. (1992) made a comparative study using density maps of  $\beta$ -alanine and 3-aminopropanal to correlate spatial structures and bond lengths; they concluded that the CO group is important for the intramolecular interactions of  $\beta$ -alanine.

McGlone & Godfrey (1995), using a Stark-modulated free-expansion jet spectrometer, observed and assigned rotational spectra of  $\beta$ -alanine in the gas phase. With the help of SCF calculations and the experimental rotational constants they asserted that the only two conformers were observed. Heal et al. (1996) investigated 20 conformers of  $\beta$ -alanine in neutral forms at the SCF level with a 6-31G\*\* basis set and analysed the shape similarities between them using the shape group method.

Rosado et al. (1997) measured vibrational spectra using Fourier transform infrared (FT-IR), Raman, matrix isolation infrared (MI-IR) spectroscopy of  $\beta$ -alanine in zwitterionic and neutral forms. Some vibrational frequencies of  $\beta$ -alanine showed remarkable differences when measured in the crystalline state and in an argon matrix at low temperatures, in the latter they are found in neutral form. A photoionization mass spectroscopy study (Jochims et al. 2004) of 5 amino acids including  $\beta$ -alanine reported fragmentation patterns, ion appearance energies and ionization energies, but the composition of conformers in gas phase was not known.

Galano & Alvarez-Idaboy (2005) optimized 12 geometries of isolated  $\beta$ -alanine using second-order Møller-Plesset perturbation theory (MP2) at the MP2/6-311G(d,p) and MP2/6-311++G(d,p) levels of calculation. High-level calculations with diffuse basis functions confirmed the importance of these kind of basis functions for describing intramolecular interactions and predicting correct relative energies, as well other molecular properties. Tian (2006) optimized geometries of 10 low-lying conformers of  $\beta$ -alanine using density functional theory (DFT) at the B3LYP/aug-cc-pVDZ level. Energetic calculations were performed, such as, stability order and ionization potential (IP) and on some radical cations; the relevance of different types of hydrogen bond was considered to interpret the electronic molecular structure of the neutral conformers. This study simulated a theoretical photoelectron spectra (PES) and indicated the existence at least three gauche conformers (G1, G2 and G3) in the gas phase experiments. However, Tian & Yang (2007) reported theoretical photoionization dynamics where only two conformations, G1 and G2, were examined and they affirmed that thermostatic temperatures affect significantly molecular fragmentations induced by photoionization. Sanz et al. (2006) observed and characterized the 4 lowest-energy conformers of  $\beta$ -alanine in a supersonic jet using a laser ablation molecular beam combined with Fourier transform microwave spectroscopy. They performed calculations on the 20

lowest-energy conformers using MP2 with a 6-311++G(d,p) basis set and determined spectroscopic parameters; by comparison with experimental results they assigned two further conformers beyond the two conformers identified previously by McGlone & Godfrey (1995). The conformers observed were I, II, III and V, following the nomenclature of Ramek (1990).

Dobrowolski et al. (2008) measured FT-IR spectra of  $\beta$ -alanine in a low-temperature argon-matrix for the first time. To interpret these spectra they optimized the ten low-energy conformations at MP2/aug-cc-pVTZ and quadratic configuration interaction singles and doubles (QCISD)/aug-cc-pVDZ level of theory. To analyse conformer abundances they used total energies calculated at the QCISD level with an aug-cc-pVDZ basis with a correction to get relative Gibbs free energies at 298.15 K. The composition found was 40% in the lowest energy conformer I, 15% in IV, II, IX and around 5% in X, while the populations conformers VIII, VI, V, III, and VII each did not exceed 3.2%. Photoionization mass spectra and photoionization efficiency spectra were obtained using laser desorption and vacuum ultraviolet (VUV) synchrotron radiation by Zhang et al. (2009a), who considered 3 neutral conformers of  $\beta$ -alanine to which they attributed pathways with conformation-specific dissociation channels to generate the fragment ions observed in the experiment.

Ribeiro da Silva et al. (2010) reported an experimental and theoretical thermochemical study of  $\alpha$ -alanine and  $\beta$ -alanine conformers where the Gibbs free energies of formation were calculated to estimate the population in the gas phase at 298.15 K. The composition for the  $\beta$ -alanine was 44.6% in the lowest-energy conformer I, 12.9% in II/VI and 9.9% in V, 6.9% in VI and 5.5% of conformer A and other minor contributions. According to their calculation the structures of conformers II and VI converge to the same minimum. Conformer A was not predicted to be one of the 20 low-energy structures listed by Ramek (1990). Dobrowolski et al. (2011) calculated the nuclear magnetic resonance (NMR) parameters of 10  $\beta$ -alanine conformers in gas phase using DFT at the B3LYP/aug-cc-pVTZ-su-1 level to correlate with chemical structure of the conformers and predict their population in the gas phase. The abundances estimated based on relative Gibbs free energy computed at the QCISD/aug-cc-pVDZ level were around 40% of  $\beta$ -alanine to the conformer I, 15% for IV, II, IX, 5% for X and not greater than 3.2% for each of VIII, VI, V, III.

Stepanian et al. (2012) performed a complete *ab initio* potential energy surface scan at the MP2/aug-cc-pVDZ level and found 20 stable  $\beta$ -alanine conformers. However, based on criteria such as high stability due to relative energies and low barriers to interconversion, they proposed that only 5 stable structures of  $\beta$ -alanine should exist in low-temperature argon matrices. By analysis of experimental FT-IR spectra and with support from UV irradiation results, they affirmed that 4 conformers were definitely identified, namely conformers I, II, IV and V. Their predicted populations in argon matrix for the 5 conformers I, II, IV, V and VII, estimated based on the relative Gibbs free energies at 420 K and the conformational interconversion barriers, are 48.1%, 23.7%, 16.8%, 3.2% and 8.2%, respectively. These populations are in good agreement with the

estimated experimental populations in argon matrices based on the intensities of spectral bands, except for conformer VII which was detected in trace amount. The Gibbs free energies were computed at the "gold-standard" coupled-cluster singles and doubles plus perturbative triples with complete basis set [CCSD(T)/CBS] level for 11 lower-energies  $\beta$ -alanine conformers whose population was estimated.

Wong et al. (2015) used a FT-IR matrix isolation spectroscopy technique to determine the composition and populations of  $\beta$ -alanine conformers in solid parahydrogen and compared their results with their own measurements in argon matrix. They performed DFT calculations of the vibrational wavenumbers and intensities of eleven low-energy conformers at the B3LYP/aug-cc-pVTZ level to assign the spectra. Five conformers were identified in the parahydrogen matrix, namely I, II, III, IV and VII; conformer III was observed in a matrix environment for the first time. Only four conformers, I, II, IV and VII, were assigned in argon matrix, however conformer V was not observed in either the argon or the solid parahydrogen matrices in their measured spectra, in contrast to the previous results of Stepanian et al. (2012). Wong et al. (2015) also discuss the population of  $\beta$ -alanine in the gas phase based on the relative Gibbs free energies at 390 K.

In this work, we have studied the 10 lowest-energy conformers of  $\beta$ -alanine. The conformers are labelled as I to X, following the nomenclature of Ramek (1990). We used the geometries of  $\beta$ -alanine conformers optimized by Stepanian et al. (2012) who carried out a complete potential energy surface search at the MP2/aug-cc-pVDZ level of theory. These geometric parameters are available in the supplementary material as table SM1. To obtain the cross sections we have described the wave functions and other properties of conformers I to X at Hartree-Fock (HF) level using 6-311G\* basis in the R-matrix calculations. Although Stepanian et al. found 20 stable conformations in their potential energy surface scan, we consider only 10 conformers of  $\beta$ -alanine due to their lower relative energies. These conformers are the ones predicted to have a significant gas-phase population at the temperatures considered. While the results of the studies discussed above do not uniformly agree on the temperature-dependent population of different  $\beta$ -alanine conformers, there are some aspects of broad agreements. Below we consider the role conformers I to X and use populations proposed by Dobrowolski et al. (2008), Ribeiro da Silva et al. (2010), Wong et al. (2015) and Stepanian et al. (2012) to construct thermally-averaged results.

### 3. Calculations

#### 3.1. The R-matrix method

Calculations of elastic collision cross sections for low-energy electrons with  $\beta$ -alanine molecules in the gas phase used the UKRMol implementation of the UK molecular R-matrix codes due to Carr et al. (2012). This method is described in details in somewhere else by Gillan et al. (1995) and Tennyson (2010), here we only present an outline of the

methodology of calculation.

In the R-matrix method the space is divided in two regions: the inner and outer region. The inner region is a sphere of radius  $a$  around the target molecule centre-of-mass, which is defined assuming that the whole electronic density of the molecular target is inside this sphere. Here a radius of  $a = 10a_0$  was found to be sufficient. When the scattering electron is inside the sphere, the interactions with the  $N$ -electrons of the target are more important and we have to consider exchange, correlation and polarization between them. The wave function of  $(N + 1)$ -electron system inside the sphere is given by

$$\begin{aligned} \Psi_k^{N+1}(x_1 \dots x_{N+1}) = & \mathcal{A} \sum_{ij} a_{ijk} \phi_i^N(x_1 \dots x_N) u_{ij}(x_{N+1}) \\ & + \sum_i b_{ik} \chi_i^{N+1}(x_1 \dots x_{N+1}) \end{aligned} \quad (1)$$

where  $\phi_i^N$  are the electronic wave functions of the target in the  $i^{\text{th}}$  state and  $u_{ij}$  is a one-electron continuum wave function, which are expanded in partial waves up to some maximum value of  $\ell$ ,  $\ell_{\text{max}}$ ;  $\mathcal{A}$  is an antisymmetrization operator which ensures that the  $(N + 1)$ -electrons are indistinguishable in the inner-region. The second summation in Eq. (1) contains  $L^2$  configurations  $\chi_i^{N+1}$  which involve placing the scattering electron in target orbitals; these configurations are used to include target polarization effects.  $a_{ijk}$  and  $b_{ik}$  are coefficients determined variationally using a specially adapted code (Tennyson 1996).

To include polarization effects we performed a systematic study including up to 30 virtual orbitals from the SCF calculation to generate two particle, one hole (2p,1h)  $L^2$  configurations, in singlet and triplet excited target states, in the second sum of Eq. (1). These calculations are generally called static-exchange-polarization (SEP); this number of virtual orbitals is also enough to converge simpler static-exchange (SE) calculations.

In the outer region it is not necessary take into consideration exchange and correlation effects, and a set of one-electron, coupled, second-order differential equations are solved to get the scattering observables as a function of electron collision energy.

As  $\beta$ -alanine conformers have permanent dipole moments, the long-range interaction is take into account using a Born closure procedure. In the R-matrix methodology the continuum orbitals are expanded up to partial waves of  $\ell_{\text{max}}$ , here  $\ell_{\text{max}} = 4$ , and the higher partial waves are included in scattering T-matrices via analytic Born T-matrices, where the rotating dipole approximation is used to calculate rotational motion to avoid the divergence of nuclei fixed approximation (Padiyal et al. 1981, Morrison 1988). Here final elastic cross sections are computed using the code POLYDCS (Sanna & Gianturco 1998) which sums rotational excitations cross sections ( $J = 0 \rightarrow J' = 0, 1, 2, \dots$ ) to convergence to allow computed cross sections be compared with measured cross sections which are generally rotationally-unresolved. Table SM2 in the supplementary material presents the rotational constants used in this work.

The systematic study to compute cross sections for each conformer broadly followed

the strategy used in our previous studies (Fujimoto et al. 2012, Fujimoto et al. 2014). These studies provide more details of calculations such as, tests of R-matrix radius, number of virtual orbitals etc. We also previously performed R-matrix calculations on averaged cross sections of  $\alpha$ -alanine conformers in gas phase (Fujimoto et al. 2016) and demonstrated that the cross sections of the thermal mixture can be very different from the cross sections of the lowest-energy conformer. This is particularly true if the permanent dipole of some conformer is very different from that of the lowest-energy conformation and the relative population of this conformer is significant. Here we executed similar study for  $\beta$ -alanine, but some differences in methodology that we make clear below.

### 3.2. Populations of conformers

In this study we consider only the 10 lowest-energy conformers which are cited in works of Dobrowolski et al. (2008), Ribeiro da Silva et al. (2010), Stepanian et al. (2012) and Wong et al. (2015). Although some of these works consider more than 10 low-energy conformers, these higher-energies conformers are generally predicted to be less important. Therefore, we choose only the 10 lowest-energy conformers that are considered to have significant thermal population, for calculating the averaged cross sections.

Our description of the isolated targets used in the R-matrix calculations was performed at the SCF or Hartree-Fock level. It is well-known that small relative energies cannot be computed reliably enough at this level to estimate the Boltzmann populations (Császár 1996, Fujimoto et al. 2016). Therefore we choose to use calculated energetic data of the above authors for two reasons: 1) the relative energies are calculated using higher levels of correlation; 2) they present Gibbs free energies which are evaluated at temperatures near experimental conditions; these correct the relative total energies which are calculated at 0 K. This correction affects the stability order of the  $\beta$ -alanine conformers as shown by Stepanian et al. (2012) in their Figure 6(a), where significant differences in the relative stability of conformers when the temperature varies from 12 K to 500 K can be seen. For example, conformer V is the second lowest-energy at 12 K and unlike most conformers, its Gibbs free energy increases with temperature and at 500 K it is the ninth lowest-energy conformer. This indicates that the relative populations show a strong dependence on temperature and that the relative stability order could be very different at different temperature. For example, conformer V has relative Gibbs free energy of 1.71 kJ/mol at 12 K and 4.88 kJ/mol at 420 K.

Our previous work (Fujimoto et al. 2016) used the relative energies of conformers of  $\alpha$ -alanine to estimate its temperature-dependent composition in the gas phase with the relative energies kept constant with temperature at their 0 K values. Comparison of the averaged cross sections which accounted for theoretical populations showed good agreement with measured populations. However, in this work we use the temperature-corrected relative Gibbs free energies calculated by Dobrowolski et al. (2008) and Ribeiro

da Silva et al. (2010) at 298.15 K, by Wong et al. (2015) at 390 K and by Stepanian et al. (2012) from 298.15 to 500 K to estimate the relative population. Stepanian et al. (2012) calculated the relative Gibbs free energies in the range 12 K to 500 K. Table 1 presents relative populations for the 10 lowest-energy conformers. Our populations differ slightly from those given in the original papers in the cases where the original work considered more than ten conformers.  $\beta$ -alanine starts to sublime near 360 K and decompose above 400 K, depending on the condition which the experiment is conducted. Thus, we have calculated averaged cross sections for populations between 298 and 500 K because we expect that the measurement of cross sections would be performed at this range of temperature.

Table 1 also presents our computed dipole moment for each conformer. We note that while each conformer possess a permanent dipole, that of conformer V is significantly bigger than for the other conformers. Table 1 compares our calculated dipole moments at the HF/6-311G\* level with results of McGlone & Godfrey (1995) obtained at the HF/6-31G\*\* level. Good agreement is found; the small discrepancies can mainly be attributed to our use of geometries optimized by Stepanian et al. (2012) in at the MP2/aug-cc-pVDZ level of theory.

### 3.3. Averaged cross sections

We have calculated cross sections for each of conformers with R-matrix method. The averaged integral or differential cross sections for 10 lowest-energy conformers weighted by population ratio is given by

$$(\text{CS})^{\text{avg}}(T) = \sum_i c_i(T)(\text{CS})_i \quad (2)$$

where the  $c_i(T)$  are the temperature-dependent population ratios and  $(\text{CS})_i$  is the SEP DCS or ICS of  $i^{\text{th}}$  conformer.

## 4. Results and discussion

Here we show our results for elastic electron  $\beta$ -alanine collisions in the gas phase at energies from 1 to 10 eV and calculated at the SEP level including 30 virtual orbitals. The results comprise eigenphase sum, resonance positions, integral cross sections (ICS) and differential cross sections (DCS) individual conformers as well as the averaged ICS and DCS weighted by population ratios.

### 4.1. Eigenphase sums and resonance features

Figure 2 exhibits eigenphase sums for the 10 lowest energy conformers I to X of  $\beta$ -alanine. The behaviour of the eigenphase sums allows us to detect the existence of resonance features. The automated detection and fitting procedure implemented by

**Table 1.** Permanent dipole moments and various relative Boltzmann population ratio sets temperature-corrected for 10  $\beta$ -alanine conformers at temperatures from 298.15 to 420 K.

Conformer	Dipole Moment, $D$		Relative Population ratio				
	our	MG	D-298 K	R-298 K	W-390 K	S1-420 K	S2-Ar
I	1.2601	1.2	0.410817	0.480389	0.225041	0.252527	0.481
II	2.6715	2.6	0.130378	0.091222	0.148407	0.153213	0.237
III	3.0168	3.0	0.022159	0.033387	0.027639	0.033709	
IV	1.5503	1.4	0.159649	0.073910	0.140827	0.106012	0.168
V	7.2728	6.8	0.022536	0.106261	0.052331	0.062471	0.320
VI	1.7809	1.1	0.024110	0.091222	0.085979	0.080796	
VII	2.7829	2.8	0.015811	0.040356	0.129176	0.077521	0.820
VIII	2.9740	3.1	0.032123	0.035469	0.033670	0.131596	
IX	1.8669	2.1	0.132598	0.023410	0.074838	0.060067	
X	1.9798	1.7	0.049819	0.024374	0.082092	0.042088	

our - dipole moment calculated in HF/6-311G\*.

MG - Dipole moment calculated in HF/6-31G\*\* by McGlone & Godfrey (1995).

D is the population based on Dobrowolski et al. (2008).

R is the population based on Ribeiro da Silva et al. (2010).

W is the population based on Wong et al. (2015).

S1 is the population based on Stepanian et al. (2012).

S2 is the population predicted by Stepanian et al. (2012) in argon matrices.

Tennyson & Noble (1984), which fits resonance positions and widths to a Breit-Wigner form, was used; the results are presented in Table 2. We emphasize that the treatment of polarization effects is the same for each conformer; 30 virtual orbitals were used in each case and the resonance position and width for can be considered relatively well converged. The resonance position and width of each conformer depend on the stabilization of the temporary anion, which depends on the level of structure calculation and, in particular, the number of virtual orbitals employed rather than any variation in temperature.

Our calculations make no allowance for the rotational temperature. Tests on previous calculations for the cross sections for water (Faure et al. 2004) showed that, within the adiabatic nuclei approximation we use here, these cross sections showed negligible variation with temperatures up to 1000 K (Tennyson, 2014, unpublished).

The eigenphase sums for all conformations show basically two structures which correspond to the resonances: low-energy near 2.8 eV and higher-energy around 9 eV. Table 2 shows the position of the lower-energy resonance varies from 2.6 eV to 3.5 eV, depending of the conformer. These lower-energy resonance structures are present in all

amino acids and do not show a large energy spread because, as discussed previously (Aflatooni et al. 2001, Ptasińska et al. 2005), they are shape resonances associated with the carboxyl group where the electron is temporarily captured by the lowest unoccupied  $\pi^*$  orbital. The difference of about 0.9 eV in the resonance position may be attributed to the stabilization of  $-\text{COOH}$  group depending of the conformer as the intramolecular interactions, such as H bonding, is distinct for each of conformer. These resonances are relatively long-lived for shape resonances as can be seen by the sharp resonance whose widths vary from 0.2 to 0.5 eV. The formation mechanism for the higher-energy resonance is not well-established: it has been suggested for glycine that it could be related to core-excited resonance (Tashiro 2008) or a shape resonance associated with the  $\sigma^*$  unoccupied orbital of OH group (Scheer et al. 2007) of amino acids. These resonances are broader: the positions of higher energy resonance ranges from 8.0 eV to 9.8 eV and the widths from 1.8 eV to 3.6 eV; they are not found for all conformers.

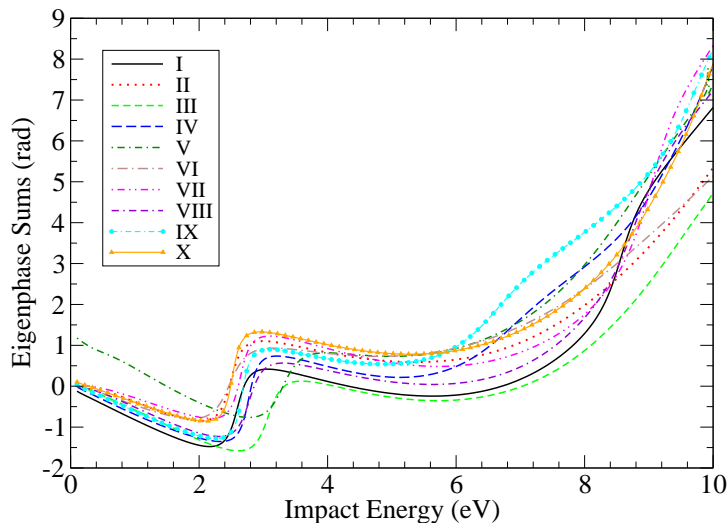


**Figure 2.** Eigenphase sums for 10 conformers of  $\beta$ -alanine computed at the SEP level.

#### 4.2. Differential cross sections

Figure 3 shows the differential cross sections (DCS) for each of 10 conformers of  $\beta$ -alanine, computed at the SEP level including Born correction, for impact energies of 1, 3, 5 and 10 eV. Table SM3 of supplementary material gives the DCS for each conformers for the energy range from 1 to 10 eV in steps of 1 eV. All the DCS exhibit similar behaviour and are of similar magnitude except for conformer V which has a much larger cross section. The main reason for this is that the conformer V has a very large permanent electric dipole which enhances the long-range interactions and results in a larger cross section. Conformer V has a dipole moment of 4.5 D, while the other conformers have dipole moments between 1.5 D and 3.5 D.

**Table 2.** Resonance parameters for 10  $\beta$ -alanine conformers: positions (widths) in eV.

Conformer	Resonance Parameters		
	position(width)	position(width)	position(width)
I	2.5955(0.2999)	8.5697(0.5213)	
II	2.4921(0.3045)		
III	3.0757(0.3854)	10.2592(0.0119)	
IV	2.7713(0.2423)	7.1150(1.8876)	
V	3.3102(0.5092)	8.9776(2.3050)	9.9219(0.0029)
VI	2.4781(0.4839)		
VII	2.6414(0.2708)	9.0447(0.5911)	
VIII	2.7833(0.3617)	8.7817(0.7672)	
IX	2.6675(0.2070)	6.7416(1.3853)	9.7470(0.9397)
X	2.5178(0.2123)	9.8645(0.8257)	

they are V, VIII, III, II and VII, have enhanced cross sections particularly at lower impact energies as seen at 1 and 3 eV of Figure 3. Basically the size of the dipole moment determine the approximate magnitude of the DCS. At 1 eV conformer V, which has a dipole moment of 7.3 D and shows the largest DCS, the conformers III and VIII are the second larger DCS with dipole near 3 D, followed by conformer II and VII which have dipole near 2.7 D. We note that issues with measurements at forward scattering angles means that measurements do not always fully reflect the importance of dipolar effects in elastic cross sections (Zhang et al. 2009b).

We compute averaged differential cross sections whereby the individual DCS of each of 10 conformers were weighted by their population ratio and summed. The population ratios were taken from the literature for temperatures of 298.15 K (Dobrowolski et al. 2011, Ribeiro da Silva et al. 2010), 390 K (Wong et al. 2015) and 420 K (Stepanian et al. 2012). All these authors have estimated the population ratio using the Gibbs free energy temperature-corrected. Figure 4 plots the averaged DCS for the sets of Dobrowolski et al. (2011) (D), Ribeiro da Silva et al. (2010) (R) at 298.15 K, Wong et al. (2015) (W) at 390 K and also two sets from Stepanian et al. (2012), one is theoretical (S1) and the other deduced to be found in argon matrix (S2). The S2 set contains only the 5 conformers that were used by Stepanian et al. (2012) to assign their argon matrix FT-IR spectra, namely conformers I, II, V, IV and VII. Despite the differences in the population, we find that the averaged DCSs are rather similar and are all larger than the DCS of the lowest-energy conformer I; this contrast is increased at lower collision energies. At higher energies near 10 eV all the averaged sets become very close and difference to the DCS of conformer I is also reduced. Comparisons with the Figure 3 it can be concluded that even though the DCS of conformer V is much bigger than other conformers, the population this conformer is small at the temperatures considered and

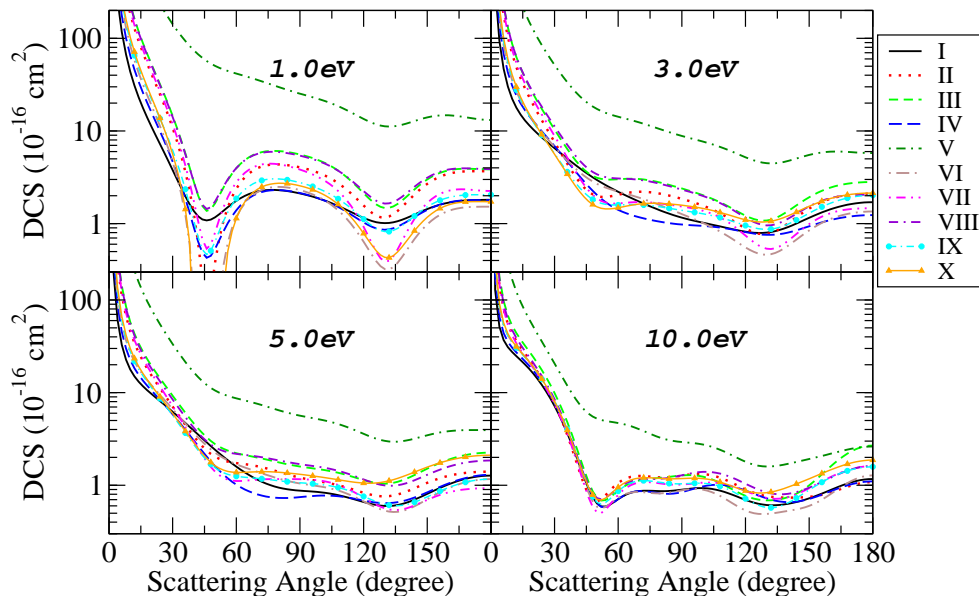


**Figure 3.** Elastic differential cross sections for electron collision with  $\beta$ -alanine conformers for impact energies at 1, 3, 5 and 10 eV. Results are for SEP calculations including Born correction.

consequently this conformer does not contribute significantly to the average.

To evaluate the effects of temperature on the averaged cross sections we used the relative Gibbs free energies due to Stepanian et al. (2012), who calculated them at temperatures ranging from 12 K to 500 K, to estimate the temperature dependence of population ratio. As their electronic structure calculations for the conformers were all performed the same high level of theory (CCSD(T)/CBS), the comparison should be even handed. We used population ratios at temperatures of 298.15 K, 390 K, 420 K and 500 K to computed conformer-averaged cross sections; these are near the conditions where the measurements could be carried out considering the sublimation temperature of  $\beta$ -alanine. The results are presented and compared in Figure 5. Table 3 shows the population ratios for temperatures of 298.15 K, 390 K, 420 K and 500 K based on relative Gibbs free energies as calculated by Stepanian et al. (2012) but considering only 10 conformers of  $\beta$ -alanine. The relative population of conformer I decrease from 38.2% up to 20.5% as the temperature increase. The proportion of conformer II also reduces from 17,0% to 13.9%. Conformer V, which has a very large dipole, decrease its relative population from 9% to 5% when the temperature increases from 298.15 to 500 K. In general, the population ratio of all other conformers, increases with temperature. Figure 5 shows that as the temperature increases the averaged DCS decreases for all

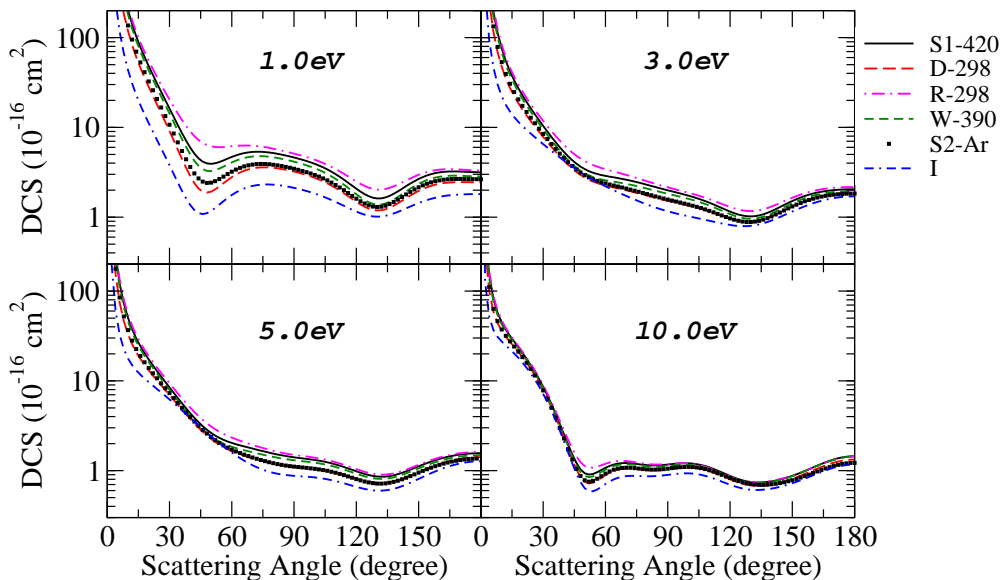


**Figure 4.** Comparison between averaged Born-corrected DCS using different sets of population ratio at different temperatures of 298.15, 390 and 420 K. The population sets are from Dobrowolski et al. (2011) (D), Ribeiro da Silva et al. (2010) (R) at 298.15 K, Wong et al. (2015) (W) at 390 K and also two sets from Stepanian et al. (2012) one is theoretical (S1) and another found in argon matrix (S2). The results are presented for impact energies of 1, 3, 5 and 10 eV; for comparison the DCS for conformer I is also given.

impact energies. This is mainly due to the decreasing relative population of conformer V. For a 1 eV impact energy the averaged DCS decreases by around 20% as the temperature varies from 298.15 to 500 K. For impact energies near 10 eV the difference is around 10% or less. The averaged cross sections is higher than that for conformer I at all impact energies, because the relative population of conformer I reduces as the temperature increases and the contributions of conformers II, III, VII and VIII, which have larger dipole moments than conformer I, become relatively more important. From these results we can conclude that even though conformer I, the lowest-energy structure, gives the largest contribution to the composition in the gas phase, it is expected that the averaged cross sections will be larger than the conformer I cross section at all temperatures were electron collisions are likely to be important.

In our previous work on electron collisions with  $\alpha$ -alanine (Fujimoto et al. 2016) we used relative (0 K) energies from electronic structure calculations instead of the temperature-corrected relative Gibbs free energy to calculate the Boltzmann population ratio. For  $\alpha$ -alanine our predicted averaged cross sections used theoretical populations

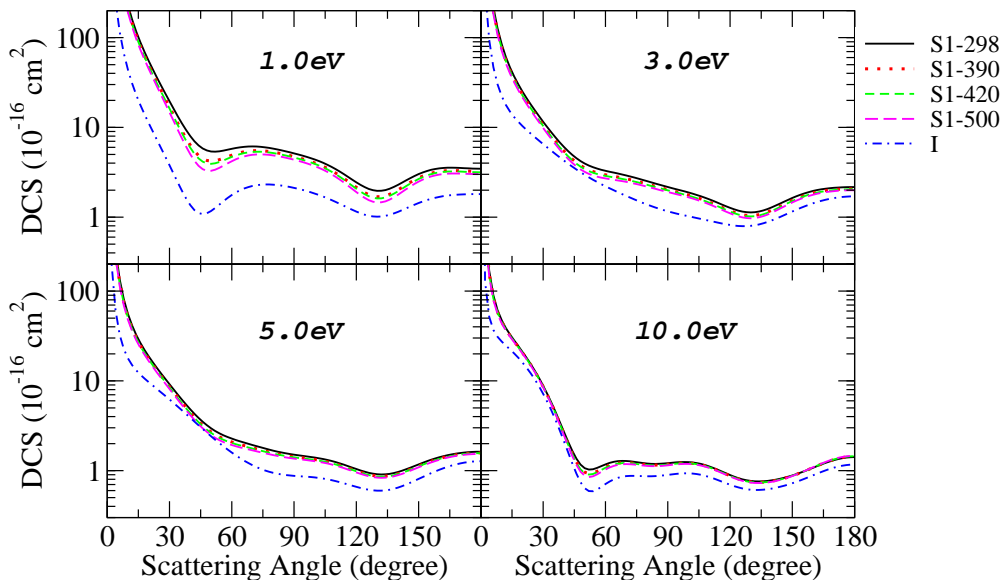


**Figure 5.** Temperature-dependence in averaged Born-corrected DCS using population ratio at temperatures of 298.15, 390, 420 and 500 K. The population set is S1 from Stepanian et al. (2012). The results are presented for impact energies of 1, 3, 5 and 10 eV; results for pure conformer I are also given.

based on the CCSD(T) electronic structure calculations which are in reasonable agreement with populations deduced from experiment (Farrokhpour et al. 2012). Figure 6 presents a comparison between our averaged DCS, SEP including Born correction for  $\beta$ -alanine, weighted with population ratios estimated from relative energies and obtained using Gibbs free energy for temperatures of 298.15 K and 420 K. The three population sets are based on the calculations of Stepanian et al. (2012): S1 is based on Gibbs free energies; RE is based on zero-point vibration energy (ZPVE) corrected relative energies and S2-Ar are population ratios predicted to exist in argon-matrix. To calculate the relative population in the RE set we used the zero-point vibration energy (ZPVE) corrected relative energies of Stepanian et al. (2012) calculated at the B3LYP/aug-cc-pVTZ level and presented in the Table 2 of their paper. When using relative energies, the order of stability is preserved for all temperatures, although the relative composition, i.e. Boltzmann population ratio, is temperature dependent. These population ratios are valid for molecules whose relative energies do not vary significantly with temperature.

The use of relative energies in RE set, equivalent to the 0 K energies with no temperature-dependent entropy contribution, gives larger cross sections mainly because

**Table 3.** Temperature-dependence of relative population ratio based on Stepanian et al. (2012) results for 10  $\beta$ -alanine conformers.

Conformer	Boltzmann Population Ratio			
	298.15 K	390 K	420 K	500 K
I	0.3823	0.2767	0.2525	0.2046
II	0.1707	0.1589	0.1532	0.1393
III	0.0202	0.0310	0.0337	0.0396
IV	0.0730	0.1000	0.1060	0.1165
V	0.0901	0.0678	0.0625	0.0504
VI	0.0488	0.0743	0.0808	0.0931
VII	0.0421	0.0699	0.0775	0.0936
VIII	0.1292	0.1330	0.1316	0.1265
IX	0.0259	0.0521	0.0601	0.0798
X	0.0178	0.0362	0.0421	0.0566

Population ratio was calculated by relative Gibbs free energies from Stepanian et al. (2012).

of increase in the population of conformer V, which varies from 24% to 22% as the temperature increases from 298.15 to 420 K. When the relative Gibbs free energy is considered the population of conformer V in S1 set varies from 9% to 5% for the same temperature range. As conformer V has the largest cross section, its population strongly influences the averaged cross sections. Comparison of the averaged DCS computed using the S2-Ar set shows that the use of Gibbs free energy to estimate the population in S1 set gives closer agreement than use of relative energies in RE set. We note that the averaged DCS estimated using population sets within the same approach, for example using relative Gibbs free energies (S1 set) or ZPVE relative energies (RE set), show smooth variation when the temperature varies from 298.15 K to 420 K. Therefore the approach used to estimate relative population is more significant than temperature variation. The population ratio based on ZPVE relative energies for temperatures from 298 to 500 K are presented in Table SM4 of supplementary material.

### 4.3. Integral Cross Sections

In this section we present results for ICS computed at the SEP level without and with Born correction for each of 10 low-energy conformers of  $\beta$ -alanine, as well as the population-averaged ICS, for impact energies ranging from 1 to 10 eV. All results include 30 virtual orbitals in our calculation at SEP level.

The ICS computed without Born correction are shown in the Figure 7 for each of 10 conformers. As the long-range interaction due to the dipole moment is mainly treated in the outer region, due to the centrifugal barrier term, for partial waves up to

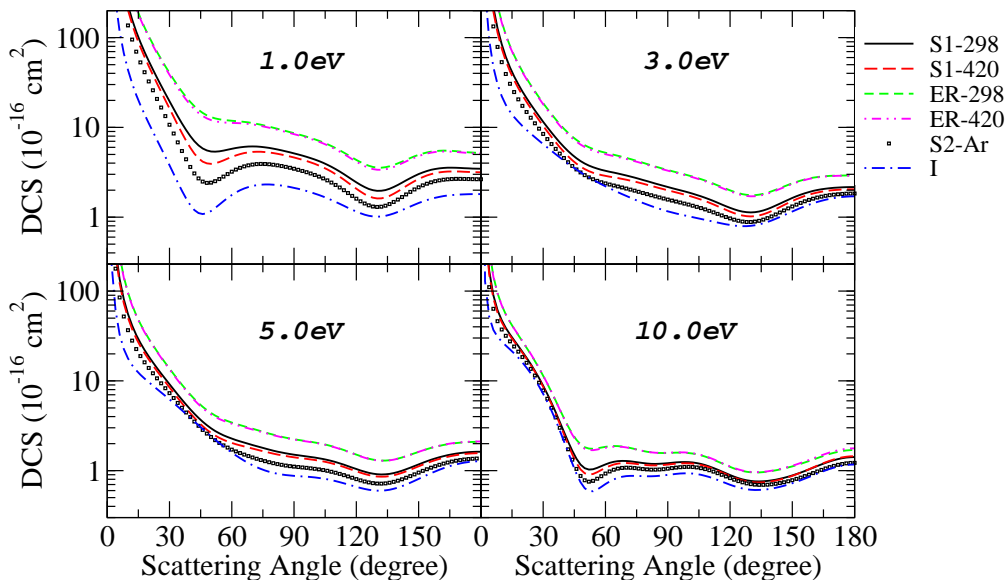
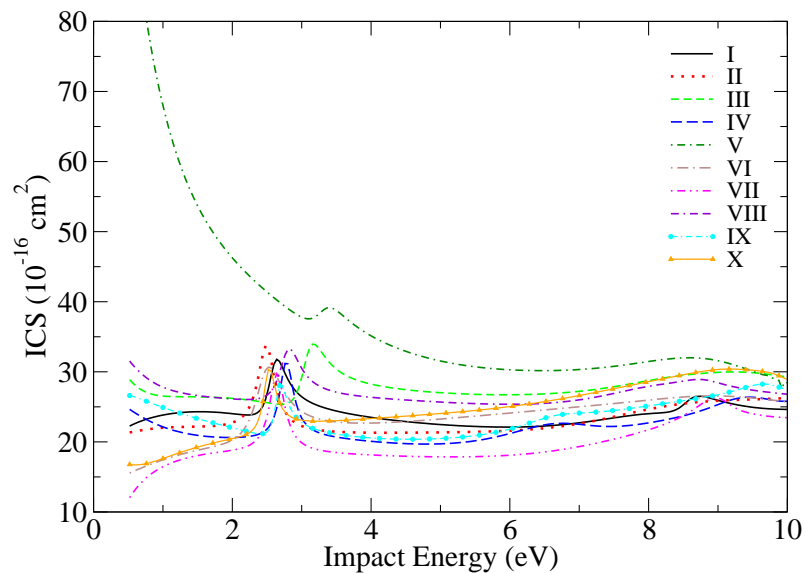


**Figure 6.** Temperature-dependence and approach-dependence in averaged Born-corrected DCS using population ratio at temperatures of 298.15 and 420 K. S1 is the population set obtained via relative Gibbs free energies; ER is the set based on ZPVE relative energies, both from Stepanian et al. (2012). Results are presented for impact energies of 1, 3, 5 and 10 eV; a comparison with pure conformer I is also given.

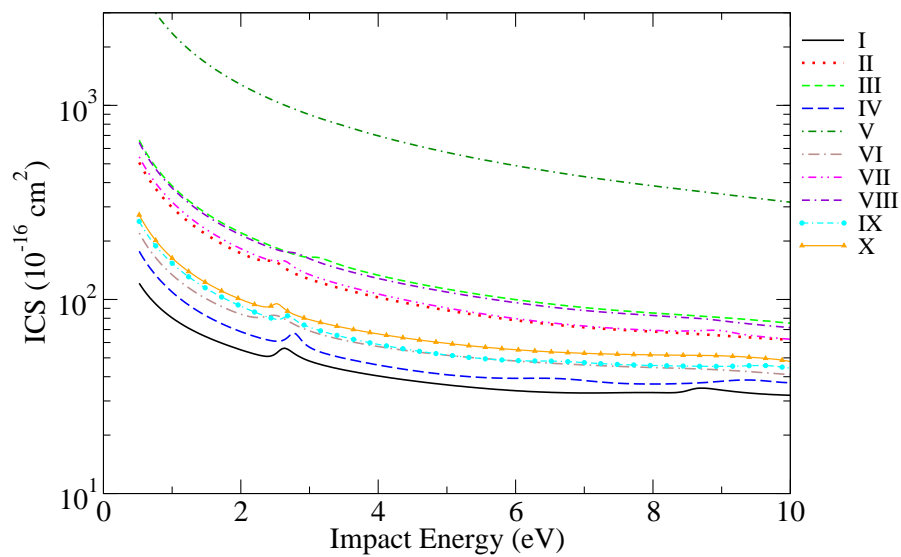
$\ell = 4$ , the resonance features is much more prominent in these results. The positions and widths of lower-energy resonance for 10 conformers can be seen in the Figure 7. The position of the resonance peaks vary from near 2.4 eV for conformer II up to near of 3.4 eV for conformer V although for the majority of the resonances peak round 2.6 eV. These low-energy resonance peaks are related to the structures observed and discussed in eigenphase sums plots in Figure 2.

Figure 8 shows our ICS results including Born correction for 10  $\beta$ -alanine conformers. Here the full long-range dipole effects are included in the calculations leading increased ICS and a smoothing out of the resonance structures. For pure dipole scattering the ICS depends on the square of the dipole moment and it can be seen that Born-corrected cross sections increase in line with the square of the calculated dipole moments presented in Table 1. As the dipoles increase the relative height of resonance peaks are diminished so much that for conformer V is no longer possible to observe the resonance features in the ICS near 3.4 eV.

Averaged ICS (SEP with Born correction) are presented in Figure 9 where various sets of Boltzmann population ratio are used. All population sets are based on relative



**Figure 7.** Integral cross section for elastic electron scattering by 10  $\beta$ -alanine conformers in SEP model with no Born correction. The low-energy resonance features are apparent.



**Figure 8.** Integral cross section for elastic electron scattering by 10  $\beta$ -alanine conformers in SEP model with Born correction.

Gibbs free energies but use different temperatures and levels of structure calculations available in the literature. The population sets are from Dobrowolski et al. (2008) (D) performed at QCISD/aug-cc-pVDZ level, Ribeiro da Silva et al. (2010) (R) at G3 level, Wong et al. (2015) (W) in B3LYP/aug-cc-pVTZ and Stepanian et al. (2012) (S1-theoretical and S2-Argon matrix) at CCSD(T)/CBS level of theory. Figure 9 shows that results computed using the R set are around 60% larger those from D set at the same temperature of 298.15 K. The key difference between the sets is the relative contribution of conformer V, which has the largest cross sections of all conformers. According to the Stepanian *et al.* calculations, the contribution of conformer V should become less important as the temperature increase, so the magnitude of ICS would be expected to decrease with temperature. However the averaged ICS using W set is higher than the results from D set, the contribution of the conformer V is near 5% for W set at 390 K and around 2% for D set at 298.15 K according to Table 2. The D and W population sets were obtained using two different methodologies which both should include a high level of correlation in their quantum mechanical calculations; however their small differences in relative population lead to significant differences in predicted thermally-averaged cross sections. The results from S1 set at 420 K are closer to those using the R set at 298.15 K while S2 at 420 K are near to the D set at 298.15 K. These results suggest that level of structure calculation has a more significant influence on the value of the relative Gibbs free energy and consequently the predicted composition than the temperature variation in the range considered.

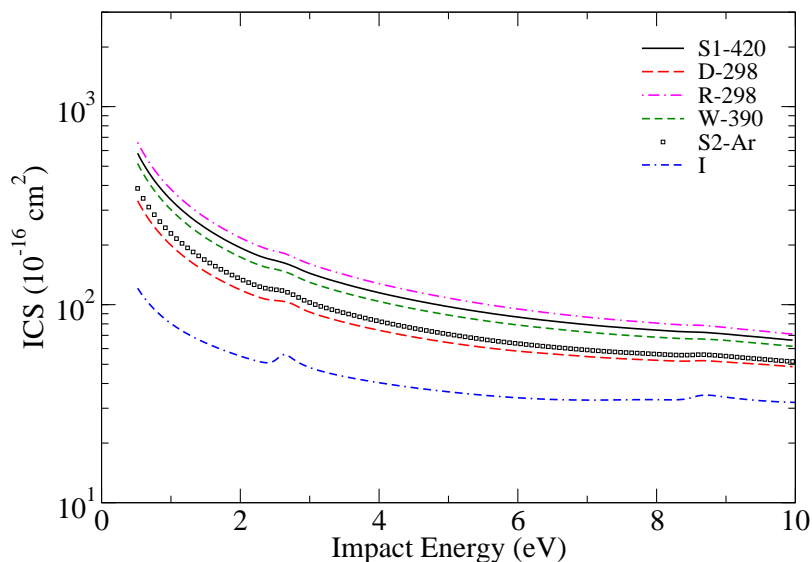


**Figure 9.** Comparison of integral cross sections, computed with SEP plus Born correction, for different population sets elastic electron scattering by  $\beta$ -alanine conformers.

The dependence on the temperature of the averaged Born-corrected SEP ICS is plotted in Figure 10. The population ratios are based on Stepanian *et al.*'s relative Gibbs free energy for conformer I to X and when the range of temperature vary from 298.15 to 500 K the ICS decrease near 20%. The explanation can be found in Table 3, where the population ratio for conformer V decrease from 9% to 5% when the temperature increase and, in general, the conformers which have higher cross sections have lower relative population so the average is going down. The comparison of ICS with conformer I shows that the average ICS can be four (lower energy) or two (higher energy) times bigger depending on the impact energy. The resonance features are smoothed in the averaged ICS compared with conformer I, although the resonance peak positions are close together.

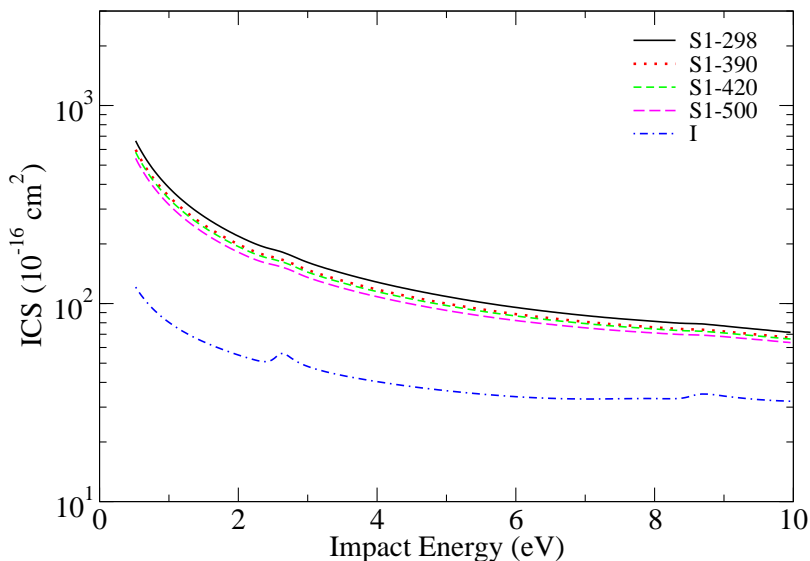


**Figure 10.** Temperature-dependence in averaged Born-corrected ICS-SEP using population ratio at temperatures of 298.15, 390, 420 and 500 K. The population set is S1 based on Stepanian *et al.* (2012) calculations. A comparison with conformer I is also presented.

Finally, to illustrate the isomer effect we compare our cross sections for  $\beta$ -alanine with our previous results for  $\alpha$ -alanine (Fujimoto *et al.* 2016). In the Figure 11 we compare the averaged-ICS-SEP with Born correction, two data sets for  $\beta$ -alanine, weighted by S1 at 403 K and S2-Ar sets, and two for  $\alpha$ -alanine, weighted by theoretical population based on relative energies (RE) calculated in CCSD(T) level at 403 K and another experimental population deduced by Farrokhpour *et al.* (2012) at 403 K. Both  $\alpha$ -alanine cross section are bigger than those for  $\beta$ -alanine, basically because the thermal composition of  $\alpha$ -alanine contains two conformers, IIA and IIB, which have relative population near 16% each and dipoles of 6.10 and 6.15 D, respectively. While the

conformer V of  $\beta$ -alanine has dipole of 7.3 D and a population near 6%. The Figure SM1 in the supplementary material gives a comparison between the DCSs  $\alpha$ - and  $\beta$ -alanine with the population sets of Figure 11.

To emphasise resonance feature, Figure SM2 of the supplementary material plots the averaged-ICS-SEP without Born correction for  $\alpha$ - and  $\beta$ -alanine with the population sets of Figure 11. The lower-resonance associated with the unoccupied  $\pi^*$  orbital of -COOH has roughly the same resonance position and width in both isomers. This indicates that the temporary anion is stabilized by a similar amount, independent of the detailed environment given by the intramolecular interactions, in  $\alpha$  and  $\beta$  isomers. This can also be seen by comparing resonance features presented in Table 2 above for  $\beta$ -alanine with Table 2 from Fujimoto et al. (2016) for  $\alpha$ -alanine.

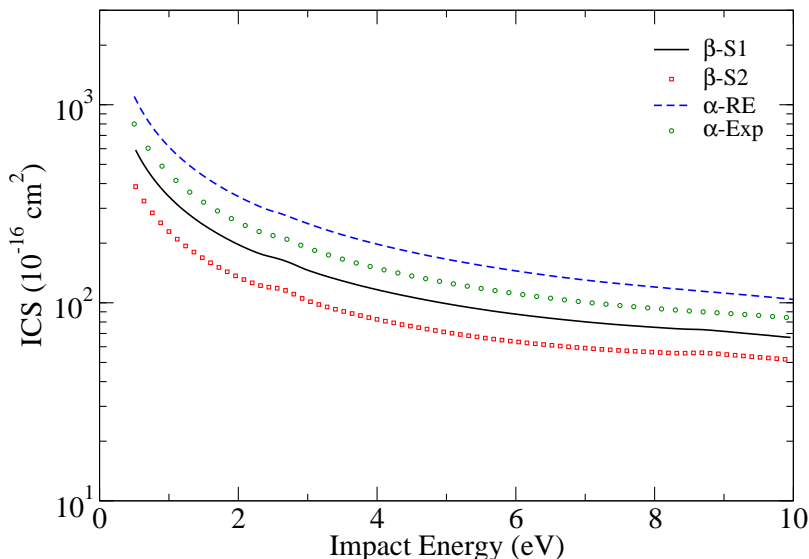


**Figure 11.** Comparison between averaged-ICS-SEP results for  $\beta$ -alanine and  $\alpha$ -alanine isomers. The population sets are: S1-403 K and S2-Ar for  $\beta$ -alanine and RE and Experimental at 403 K for  $\alpha$ -alanine conformers.

## 5. Conclusions

We present a theoretical study of elastic electron scattering by 10 gas-phase conformers of  $\beta$ -alanine. The cross sections calculations are performed with the UKRMol codes at the static exchange plus polarisation (SEP) level with 30 virtual orbitals, in the range from 1 to 10 eV impact energies. The cross sections for individual conformers are calculated and the average are take into account weighted by population ratio at a given temperature. Population ratios are obtained from relative Gibbs free energy temperature-corrected to the values near the usual experimental conditions.  $\beta$ -alanine

is solid and must be heated to be sublimed, so we considered temperatures from 298.15 K up to 500 K and used calculated relative Gibbs free energies from the literature. The eigenphase sums for individual conformers all show a low-energy shape resonance associate with occupation of the  $\pi^*$  unoccupied orbital of carboxylic group by the scattering electron. The resonance energy varies from about 2.5 eV to 3.3 eV, depending on the geometry of conformer; intramolecular interactions are responsible in difference in the temporary anion stabilities. Figure 4 compares averaged DCS and shows that cross sections estimated at 298.15 K could give averaged DCS lower than that one at 420 K depending on the population ratio set employed. However, when we compare averaged DCS calculated at different temperatures but using population ratio estimated from the same level of calculation data, the averaged cross sections reduce with increase in temperature. The reduction is around 20% as the temperature increase from 298.15 to 500 K.

Our previous study (Fujimoto et al. 2016) on  $\alpha$ -alanine used relative energies, calculated at 0 K, to estimate conformer populations near 400 K where electron-collision experiments have been conducted. In this work for  $\beta$ -alanine, we use the relative temperature-corrected Gibbs free energy available in the literature to estimate the population. We show that including the effect of entropy in the model leads to population ratios which are very different at 400 K compared to 12 K, with some conformers swapping positions in the order of abundances. These significant composition changes are reflected in changes in the temperature-dependent conformer-averaged cross sections. Although our conclusion about the dependence of the averaged cross sections on temperature is similar to that of our previous work, if we had use the same method to estimate the population (relative 0 K energies), the effects varying the temperature from 298.15 to 420 K would have been significantly less. The dipole moments of  $\beta$ -alanine conformers vary from 1.2 D to near 7.3 D. Treating these correctly requires the Born correction to our cross sections to allow for the long-range electron-dipole interactions. Our averaged cross sections are strongly influenced by the proportion of the highly polar conformer V in the given population ratio. This is the effect which makes the averaged  $\beta$ -alanine cross sections more sensitive to the methodology used than those for  $\alpha$ -alanine.

The averaged cross sections of  $\alpha$ -alanine are bigger than  $\beta$ -alanine, due to the high contribution of conformers, which have large cross sections because of large dipole moments, to the average. And also to the substantial relative population of conformers at a given temperature.

Finally, we find that the averaged cross sections are all higher the cross sections of the lowest-energy conformer I. This means that for large and flexible molecules, like amino acids and many other biomolecules, the electron impact cross sections for molecules in gas phase should consider the thermal mixture when comparisons are made with experimental measurements rather simply than lowest-energy conformer. The low-energy barriers related to the rotations of functional groups means that it is not possible to observe each conformer separately in the electron scattering cross sections measurement.

## Acknowledgements

MMF acknowledges partial support from the Brazilian agency Conselho Nacional de Desenvolvimento Científico e Tecnológico (CNPq) and EVRL for partial grant for UFPR-TN.

## References

- Aflatooni K, Hitt B, Gallup G A & Burrow P 2001 *J. Chem. Phys.* **115**, 6489–6494.
- Blagojevic V, Petrie S & Bohme D K 2003 *Monthly Not. R. Astron. Soc.* **339**, L7–L11.
- Bode M & Gordon M S 1998 *J. Mol. Graph. Model.* **16**, 133–138.
- Boudaïffa B, Cloutier P, Hunting D, Huels M A & Sanche L 2000 *Science* **287**, 1658–1660.
- Carr J M, Galiatsatos P G, Gorfinkiel J D, Harvey A G, Lysaght M A, Madden D, Masin Z, Plummer M & Tennyson J 2012 *Eur. Phys. J. D* **66**, 58.
- Choquet D & Korn H 1988 *Neurosci. Lett.* **84**, 329–334.
- Császár A G 1996 *J. Phys. Chem.* **100**, 3541–3551.
- Dobrowolski J C, Jamróz, M H, Kołos R, Rode, J E & Sadlej J 2008 *Chem. Phys. Chem.* **9**, 2042–2051.
- Dobrowolski J C, Rode, J E & Sadlej J 2011 *Comp. Theor. Chem.* **964**, 148–154.
- Ehrenfreund P, Glavin, D P, Botta O, Cooper G & Bada J L 2001 *Proc. Natl. Acad. Sci. U.S.A.* **98**, 2138–2141.
- Farrokhpour H, Fathi F & Naves De Brito A 2012 *J. Phys. Chem. A* **116**, 7004–7015.
- Faure A, Gorfinkiel J D & Tennyson J 2004 *J. Phys. B: At. Mol. Opt. Phys* **37**, 801–807.
- Fujimoto M M, Brigg W J & Tennyson J 2012 *Eur. J. Phys. D* **66**, 204.
- Fujimoto M M, Tennyson J & Michelin S E 2014 *Eur. Phys. J. D* **68**, 67.
- Fujimoto M M, de Lima E V R & Tennyson J 2016 *J. Phys. B: At. Mol. Opt. Phys.* **49**, 215201.
- Gianturco F A & Jain A 1986 *Phys. Rep.* **143**, 347–425.
- Gillan C J, Tennyson J & Burke P G 1995 in *Computational methods for Electron-molecule collisions*, edited by W. Huo, F.A. Gianturco, Plenum (New York), pp. 239-254
- Hayashi O, Nishuzuka Y, Tatibana M, Takeshita M & Kuno S 1961 *J. Biol. Chem.* **236**, 781–790.
- Heal G A, Walker P D, Ramek M & Mezey P G 1996 *Can. J. Chem.* **74**, 1660-1670.
- Juaristi, E & Soloshonok, V 2005 in *Enantioselective Synthesis of  $\beta$ -Amino Acids* (New York: Wiley, 2nd ed)
- Jochims H-W, Schwell M, Chotin J-L, Clemino M, Dulieu F, Baumgärtel H & Leach S 2004 *Chem. Phys.* **298**, 279–297.
- Kasschau M R, Skisak C M, Cook J P & Mills W R 1984 *J. Comput. Physiol. B* **154**, 181–186.
- McGlone S J & Godfrey P D 1995 *J. Am. Chem. Soc.* **117**, 1043–1048.
- Galano A & Alvarez-Idaboy J R 2005 *Arkivoc* **6**, 7-18.
- Morrison M A 1988 *Adv. At. Mol. Phys.* **24**, 51–156.
- Padial N T, Norcross D W & Collins L A 1981 *J. Phys. B* **14**, 2901–2909.
- Ptasińska S, Denifl S, Candori P, Matejcik S, Scheier P & Märk T D 2005 *Chem. Phys. Lett.* **403**, 107–112.
- Ramek M 1990 *J. Mol. Struct. (THEOCHEM)* **208**, 301-355.
- Ramek M, Flock M, Kelterer A-M & Cheng V K W 1992 *J. Mol. Struct. (THEOCHEM)* **276**, 61–81.
- Ribeiro da Silva M A V, Ribeiro da Silva M D M C, Santos A F L O M, Roux M V, Foces-Foces C, Notario R, Guzmán-Mejía R & Juaristi E 2010 *J. Phys. Chem. B* **114**, 16471–16480.
- Rosado M T S, Duarte M & Fausto R 1997 *J. Mol. Struct.* **410**, 343–348.
- Sanna N & Gianturco F A 1998 *Comput. Phys. Commun.* **114**, 142–167.
- Sanz M E, Lesarri A, Peña M I, Vaquero, V, Cortijo V, López J C & Alonso J L 2006 *J. Am. Chem. Soc.* **128**, 3812–3817.
- Scheer A M, Mozejko P, Gallup G A & Burrow P D 2007 *J. Chem. Phys.* **126**, 174301.

- Stepanian S G, Ivanov A Y, Smyrnova D A & Adamowicz L 2012 *J. Mol. Struct.* **1025**, 6–19.
- Tashiro M 2008 *J. Chem. Phys.* **129**, 164308.
- Tennyson J 1996 *J. Phys. B: At. Mol. Opt. Phys.* **29**, 1817–1828.
- Tennyson J 2010 *Phys. Rep.* **491**, 29–76.
- Tennyson J & Noble C J 1984 *Comput. Phys. Commun.* **33**, 421–424.
- Tian S X 2006 *J. Phys. Chem. A* **110**, 3961–3966.
- Tian S X & Yang J 2007 *J. Chem. Phys.* **126**, 141103.
- Tiedje K E, Stevens K Barnes S & Weaver D F 2010 *Neurochem. Int.* **57**, 177–188.
- Wong Y T A, Toh S Y, Djuricanin P & Momose T 2015 *J. Mol. Spectrosc.* **310**, 23–31.
- Zhang L, Pan Y, Guo H, Zhang T, Sheng L, Qi F, Lo P-K & Lau K-C 2009 *J. Phys. Chem. A* **113**, 5838–5845.
- Zhang R, Faure A & Tennyson J 2009 *Physica Scripta* **80**, 015301.